Expanded View Figures

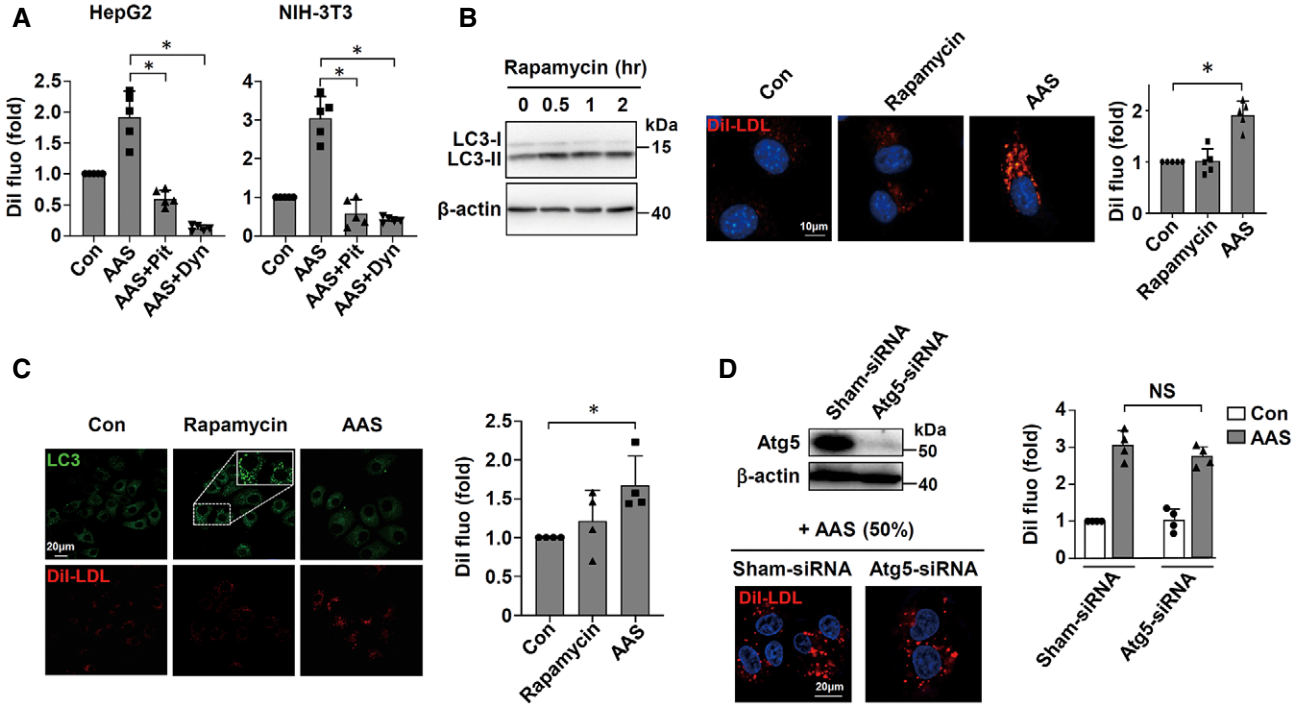

Figure EV1. AAS-stimulated LDL endocytosis was clathrin- and dynamin-dependent but autophagy-independent.

A Fluorescence microscopy data showing that AAS (50%)-stimulated DiI-LDL endocytosis was abolished by pretreatment with Pitstop2 (Pit, 20 μM) or Dynasore (Dyn, 80 μM). Con, complete culture medium.

B Western blot for LC3 (left panel, example from 6 independent experiments with similar results) and fluorescence microscopy data (right panels) showing that rapamycin (5 μM) quickly induced autophagic response in NIH-3T3 cells, but failed to modulate DiI-LDL endocytosis as compared to AAS (assayed at 120 min).

C Fluorescence microscopy images of LC3 immuno-staining and DiI-LDL uptake (left panel), and quantitative data of DiI-LDL uptake (right panel) in HepG2 cells showing that rapamycin (240 min) induced autophagy but failed to modulate LDL endocytosis, while AAS (50% for 240 min) had opposite effects. The enlarged image area shown in the insert demonstrated LC3 puncta formation in rapamycin-treated cells.

D Atg5 gene silencing (western blots: example from 4 independent tests with similar results) by siRNA transfection in HepG2 cells did not change AAS-stimulated DiI-LDL endocytosis shown by the fluorescence microscopy data.

Data information: Data were mean ± SD. *$P < 0.05$, one-way ANOVA (except for the HepG2 data in EV1A, which were examined with nonparametric Kruskal–Wallis test because of non-Gaussian distribution). NS, no significance.
Source data are available online for this figure.

© 2022 The Authors

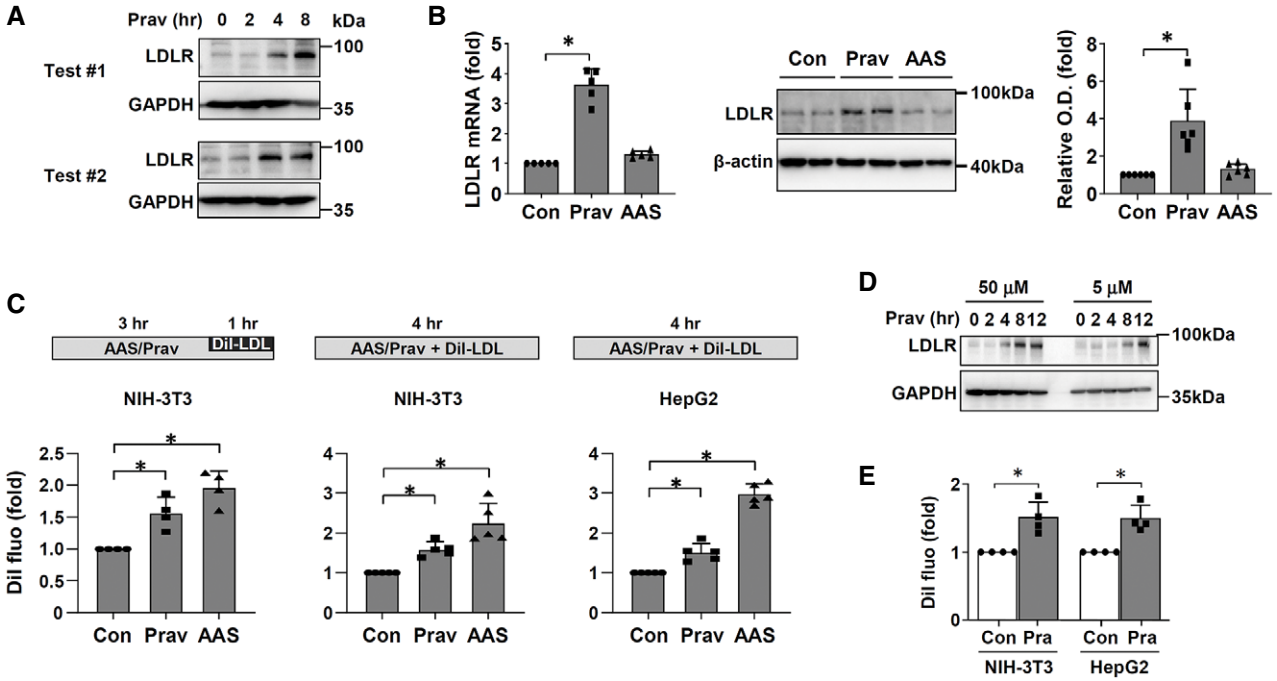

Figure EV2. AAS and pravastatin (Prav) induced comparable effects on cellular LDL uptake.

A Preliminary western blot tests showing the time course of changes in LDLR expression in response to 50 μM pravastatin treatment in NIH-3T3 cells (2 independent experiments with similar results).

B Real-time PCR (left panel) and western blotting (right panels) results showing that pravastatin (50 μM for 4 h), but not AAS, significantly upregulated the mRNA and protein levels of LDLR in NIH-3T3 cells.

C Fluorescence microscopy data showing that both AAS and pravastatin similarly enhanced DiI-LDL uptake in NIH-3T3 (Prav 50 μM) and HepG2 (Prav 100 μM) cells.

D Western blot experiments showing that pravastatin at low and high concentrations exhibited different time courses of LDLR induction (example from 4 independent tests with similar results).

E Fluorescence microscopy data showing that pretreatment with pravastatin at 5 μM for 12 h significantly enhanced DiI-LDL endocytosis.

Data information: Data were mean ± SD. *$P < 0.05$, one-way ANOVA or unpaired *t*-test as appropriate (except for the Relative O.D. data in EV2B, which were examined with nonparametric Kruskal–Wallis test because of non-Gaussian distribution).
Source data are available online for this figure.

 © 2022 The Authors

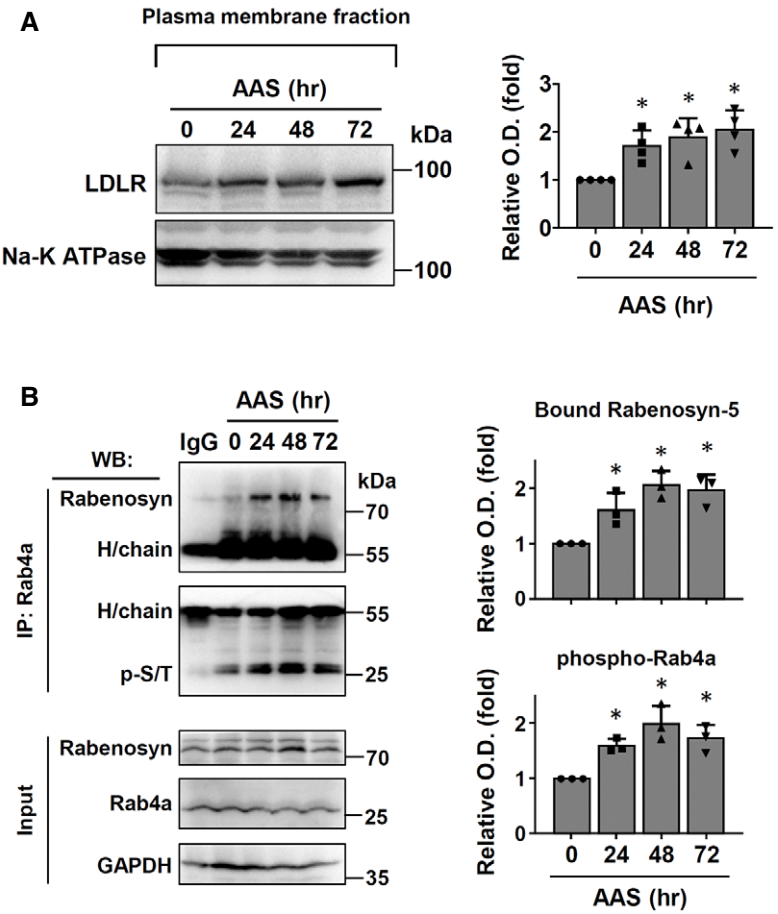

Figure EV3. Effects of acute AAS treatment *in vivo* on LDLR translocation to the plasma membrane, Rab4a phosphorylation, and Rab4a/Rabenosyn-5 interaction in the liver.

A Representative western blots and densitometry data showing that AAS increased the amount of LDLRs on the plasma membrane fraction.

B Immunoprecipitation and western blot results showing that AAS treatment *in vivo* enhanced Rab4a phosphorylation, and the interaction between Rab4a and Rabenosyn-5. H/chain, Ig heavy chain. Normal IgG was used as negative control for IP. p-(S/T), anti-phospho serine/threonine antibody.

Data information: Data were mean ± SD. *$P < 0.05$ versus baseline (0 h), one-way ANOVA.
Source data are available online for this figure.

© 2022 The Authors

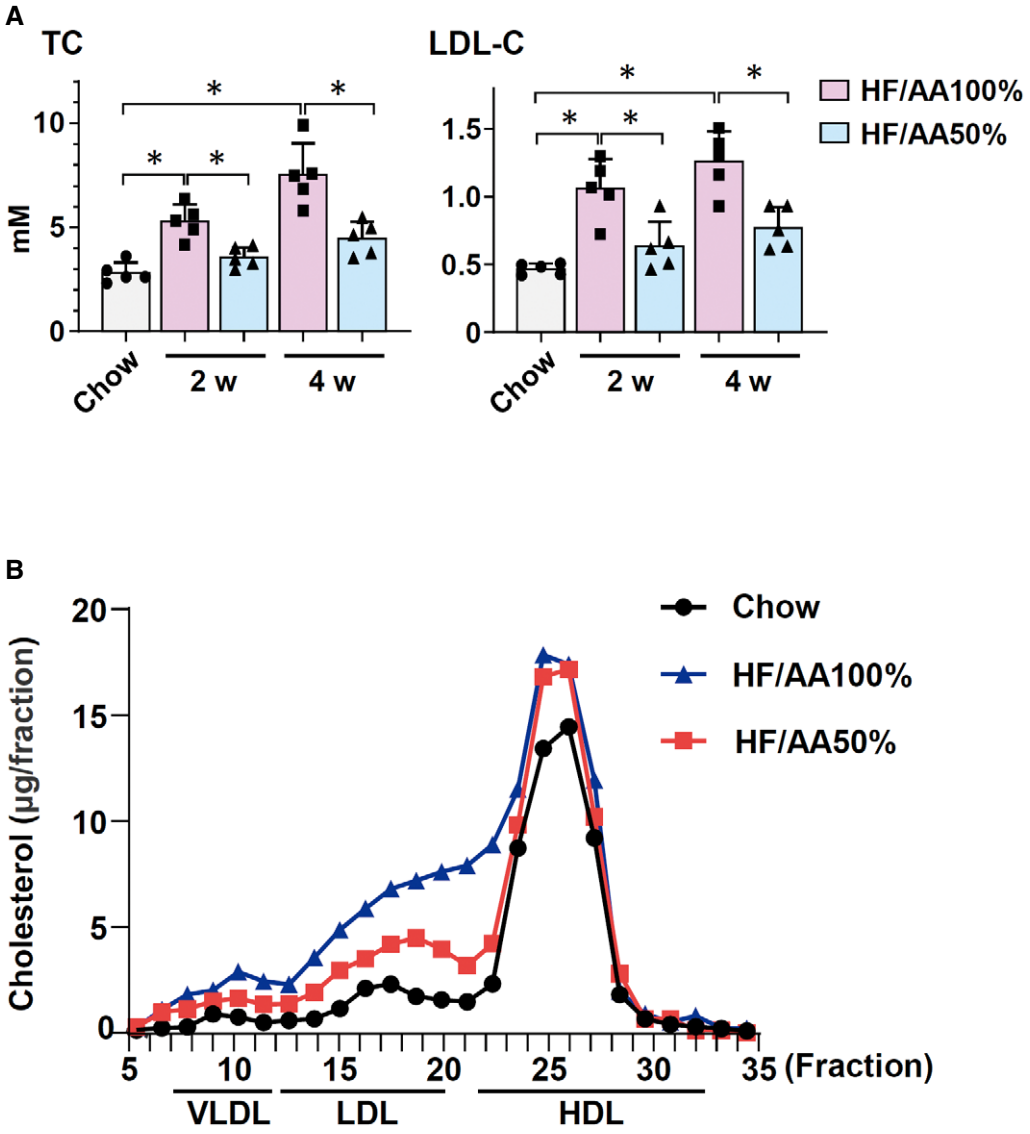

Figure EV4. Effects of dietary amino acid restriction on blood cholesterol levels in heterozygous *LDLR*$^{+/-}$ mice.

A Measurements of total cholesterol (TC) and LDL cholesterol (LDL-C) levels showing that reducing dietary amino acid content by 50% (AA50%) ameliorated high fat (HF) diet-induced hypercholesterolemia. Animals fed with chow diet were included as the baseline control.

B Fast protein liquid chromatography (FPLC) analysis of pooled plasma (n = 5 mice in each group) showing that the levels of both LDL and VLDL fractions were reduced in response to dietary amino acid restriction.

Data information: Data in panel (A) were expressed as mean ± SD. *P < 0.05, one-way ANOVA.
Source data are available online for this figure.

© 2022 The Authors

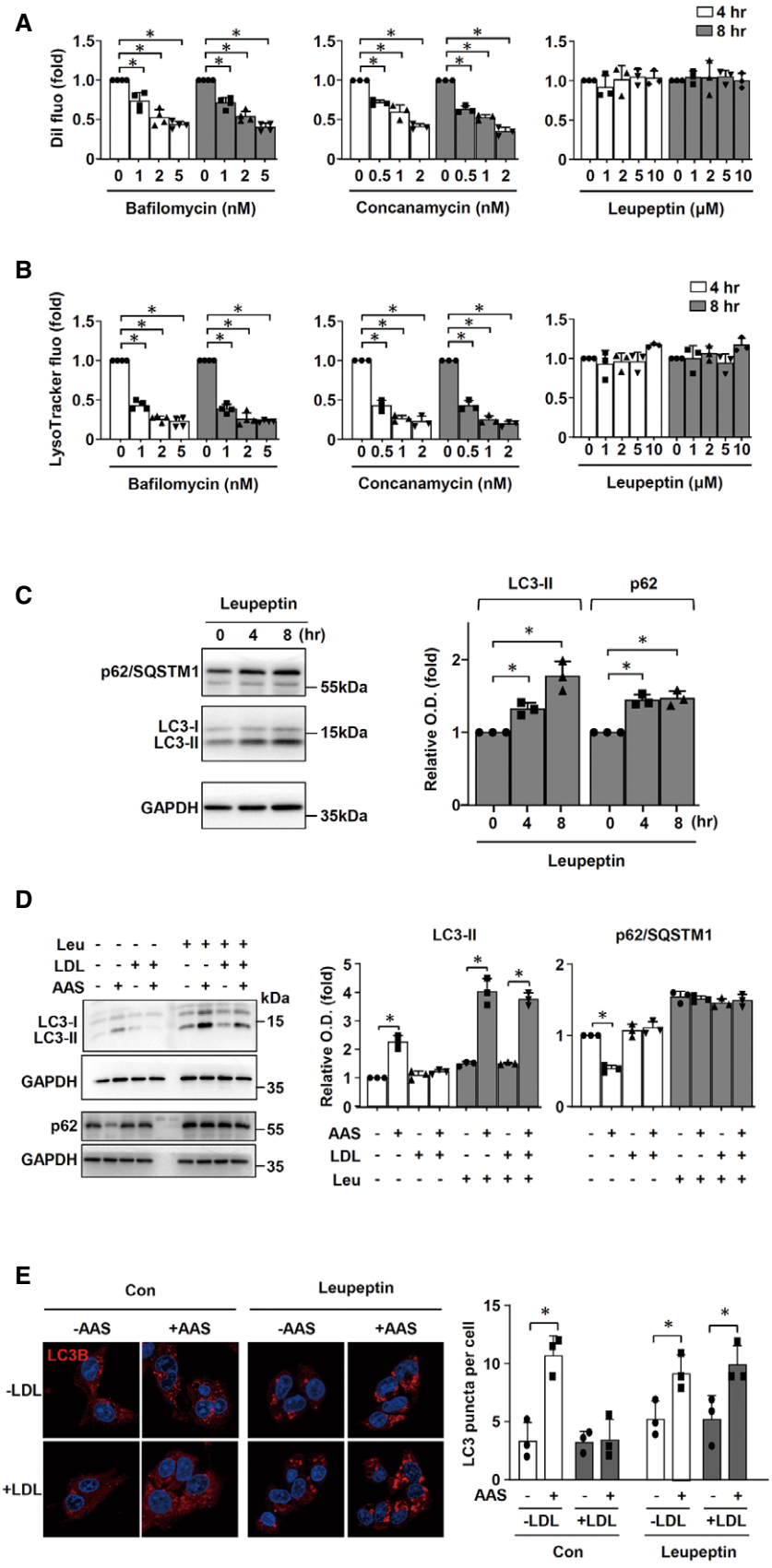

Figure EV5. Lysosome inhibition diminished the suppressive effect of exogenous LDL on AAS-induced autophagy in HepG2 cells.

A Quantitative data of fluorescence microscopy showing that pretreatment with bafilomycin A1 or concanamycin A, but not leupeptin, inhibited basal LDL endocytosis. Dil-LDL incubation was for 1 h.

B Quantitative data for LysoTracker staining assay showing that leupeptin had no effect on lysosome acidification. The v-ATPase inhibitors bafilomycin A1 and concanamycin A were used as positive controls.

C Western blots and corresponding densitometry data showing the effect of leupeptin (5 μM) on the basal autophagic activity in resting cells.

D, E Results of western blot (D) and immunofluorescence experiments (E) showing that the autophagy-inhibiting effect of exogenous LDL was diminished by leupeptin (Leu, 5 μM) pretreatment. AAS (0%) treatment was for 4 h.

Data information: Data were expressed as mean ± SD. *$P < 0.05$, one-way ANOVA.
Source data are available online for this figure.

© 2022 The Authors